Solar Hydrogen Production Using Carbon Quantum Dots and a Molecular Nickel Catalyst

Benjamin C. M. Martindale,[†] Georgina A. M. Hutton,[†] Christine A. Caputo, and Erwin Reisner*

Christian Doppler Laboratory for Sustainable SynGas Chemistry, Department of Chemistry, University of Cambridge, Lensfield Road, Cambridge CB2 1EW, U.K.

S Supporting Information

ABSTRACT: Carbon quantum dots (CQDs) are established as excellent photosensitizers in combination with a molecular catalyst for solar light driven hydrogen production in aqueous solution. The inexpensive CQDs can be prepared by straightforward thermolysis of citric acid in a simple one-pot, multigram synthesis and are therefore scalable. The CQDs produced reducing equivalents under solar irradiation in a homogeneous photocatalytic system with a Ni-bis-(diphosphine) catalyst, giving an activity of 398 μmol$_{H_2}$ $(g_{CQD})^{-1}$ h^{-1} and a "per Ni catalyst" turnover frequency of 41 h^{-1}. The CQDs displayed activity in the visible region beyond $\lambda > 455$ nm and maintained their full photocatalytic activity for at least 1 day under full solar spectrum irradiation. A high quantum efficiency of 1.4% was recorded for the noble- and toxic-metal free photocatalytic system. Thus, CQDs are shown to be a highly sustainable light-absorbing material for photocatalytic schemes, which are not limited by cost, toxicity, or lack of scalability. The photocatalytic hybrid system was limited by the lifetime of the molecular catalyst, and intriguingly, no photocatalytic activity was observed using the CQDs and 3d transition metal salts or platinum precursors. This observation highlights the advantage of using a molecular catalyst over commonly used heterogeneous catalysts in this photocatalytic system.
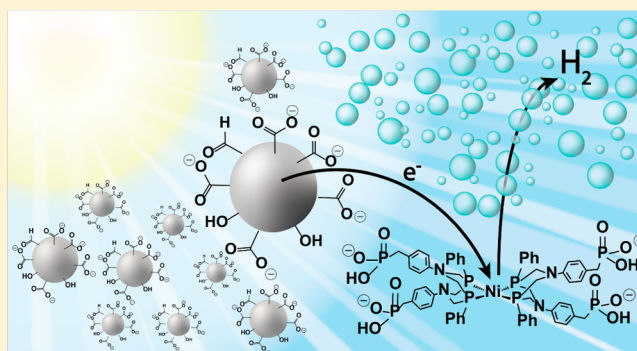
INTRODUCTION

Efficient and inexpensive photocatalytic water splitting is a major focus of research toward solar energy conversion and storage.[1−4] Photocatalytic H$_2$ production from water requires the efficient coupling of light harvesting and charge transfer with catalytic processes. Homogeneous solution-based and semiheterogeneous colloidal systems comprising a photosensitizer in conjunction with a proton reduction catalyst have attracted significant interest as a means of optimizing and combining these components.[5−10] Hybrid systems, however, typically employ photosensitizers that are either expensive (ruthenium-based dyes),[5,6] toxic (CdSe[8] and CdS[11] quantum dots), or unstable (organic dyes),[12,13] which limits their practical application. Perovskites based on lead have attracted recent attention as efficient light absorbers in solar cells and photoelectrochemical cells,[1] but they are toxic and highly unstable in water and so are currently unsuitable for aqueous systems.[14,15] Graphitic carbon nitride (CN$_x$) has been put forward as a heterogeneous photosensitizer; however, visible light absorption and interfacial charge transfer limits its efficacy.[7,16,17] Furthermore, the hydrophobicity of these organic materials often restricts their application in aqueous solution and synthetic procedures require thermal condensation at high temperatures (400−600 °C) from a limited range of nitrogen-containing precursors such as cyanamide, dicyandiamide, or melamine.[16] Despite this recent progress, there remains a need

to develop cheap, robust, and efficient photosensitizer materials for artificial photosynthetic systems.

Photoluminescent carbon nanoparticles, referred to herein as carbon quantum dots (CQDs), are a relatively new class of low cost carbon nanomaterial which has attracted recent interest for applications in bioimaging,[18] sensing,[19] and light emitting devices[20] due to their biocompatibility,[21] water solubility, and stable photoluminescence properties.[22,23] CQDs, typically 2−10 nm in diameter, predominantly consist of amorphous carbon together with nanocrystalline regions of sp^2-hybridized graphitic carbon.[24] They display strong blue photoluminescence and good optical absorption in the UV and near-visible region rendering them promising candidates as photosensitizers for photocatalytic applications. CQDs are typically terminated by carboxylic acid groups at their surface, which impart high solubility in aqueous solutions and provide potential for further functionalization. Unlike many other carbon nanomaterials, e.g. carbon nanotubes, graphene (oxide) and graphene (oxide) quantum dots,[25] CQDs are easily and inexpensively synthesized on a multigram scale by a number of simple bottom-up methods including partial oxidation of candle[26] or natural gas soot,[24] electrolysis of alcohols,[27] and low-temperature thermol-
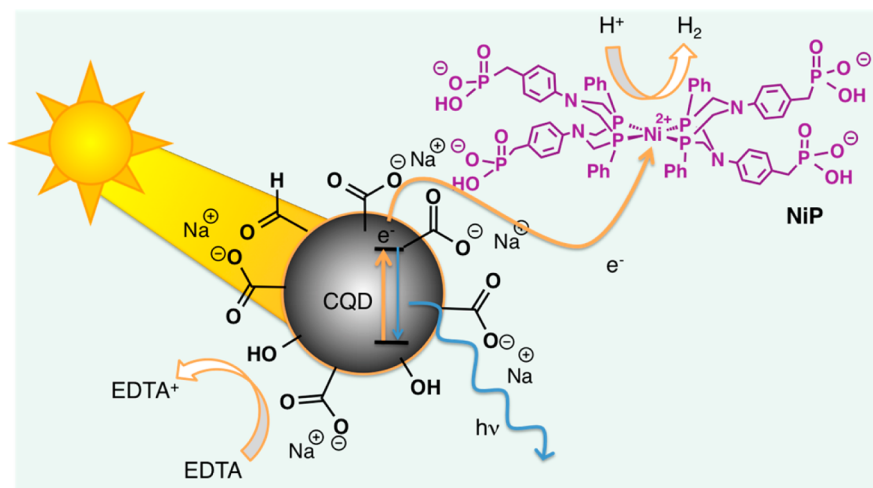
Figure 1. Representation of solar H_2 production using the hybrid CQD–**NiP** system described in this work. Irradiation of photoluminescent CQDs results in the direct transfer of photoexcited electrons to the catalyst **NiP** with subsequent reduction of aqueous protons. The electron donor EDTA carries out quenching of photoinduced holes in the CQDs.

ysis (<200 °C) of a cheap carbon source such as citric acid,[28,29] glucose,[30] and even waste products.[31−33]

While exhibiting promising light-harvesting and electron transfer properties,[34,35] CQDs have been underexplored in photocatalytic applications and have almost exclusively been used in conjunction with another photosensitizer and for photodegradation of organic dyes.[36−38] The first use of CQDs as a primary photosensitizer for fuel production was for the photoreduction of carbon dioxide to formic acid with polyethylene glycol-passivated CQDs modified with deposits of the noble metals Au or Pt.[39,40] Here, we report a solar H_2 production system using CQDs as the sole photosensitizer in combination with a molecular Ni catalyst − the first such use of CQDs in a homogeneous photocatalytic system in combination with a molecular catalyst (Figure 1).

RESULTS AND DISCUSSION

Water-soluble, carboxylic acid terminated CQDs were synthesized according to a modified procedure[28] by thermolysis of 100 g of citric acid under air at 180 °C for 40 h. Dissolution in water followed by neutralization to pH 7 with aqueous NaOH produced a concentrated brown solution of sodium carboxylate terminated CQDs. The product was isolated by freeze-drying as a yellow-orange powder in 45 g yield (for full details, see Experimental Section). The exclusive use of cheap and abundant starting materials such as citric acid, a low-cost natural product and commodity chemical produced by fermentation on the megaton scale, as well as the low operating temperature makes the synthesis of CQDs highly scalable and environmentally sustainable.

Several spectroscopic techniques were utilized to confirm the quantitative decomposition of the citric acid and to characterize the nature of the CQD product. Infrared (IR) spectroscopy (Figure S1) shows two strong features at $\tilde{\nu}$ = 1395 and 1554 cm^{-1} corresponding to the symmetric and antisymmetric stretches of the carboxylate group, consistent with the presence of this group on the surface of the dot. Significantly, the peaks are shifted from that of the sodium hydroxide neutralized form of the starting material (sodium citrate carboxylate stretches; $\tilde{\nu}$ = 1386 and 1580 cm^{-1}). ^{13}C NMR spectroscopy (Figure S2) also indicates the formation of CQDs, where a variety of new

carbon environments are present, corresponding to carbonyl (surface; δ = 170−190 ppm), sp^2 (graphitic, amorphous; δ = 120−150 ppm), and sp^3 (amorphous; δ = 10−70 ppm) carbon environments. X-ray photoelectron spectra (XPS) of the CQDs (Figure S3) show C, O, and Na (as well as Sn from the fluorine-doped tin oxide substrate) in the survey spectrum. The high resolution XPS spectrum of the C 1s region shows two strong peaks at 284.8 and 288.2 eV, which correspond to C−C and C=O environments, respectively.[27]

High-resolution transmission electron microscopy (HR-TEM) was used to determine the shape, size, and nature of the CQDs (Figure 2). They are spherical nanoparticles with an average size of 6.8 ± 2.3 nm and a relatively broad size distribution. The average particle size corresponds to an average molecular weight of about 225 kDa (see Experimental Section for calculation). Regions of both graphitic and amorphous carbon can be seen by HR-TEM (Figure S4); the graphitic regions showed lattice fringes corresponding to the (100) intralayer spacing of 2.4 Å (Figure 2).[22,41] The powder X-ray diffraction (XRD) spectrum shows a broad feature centered at 29.8° 2θ, which corresponds to a lattice spacing of 3 Å, similar to the (200) reflection (d_{002} = 3.4 Å) of disordered graphitic-like species (Figure S5).[42,43] The low signal-to-noise ratio is consistent with a significant portion of the sample being amorphous.

The optical properties of the CQDs were investigated by UV−vis and photoluminescence (PL) spectroscopy (Figure S6). The UV−vis spectrum presents a broad absorption in the UV region with a tail in the near-visible region, which has been attributed to various $\pi−\pi*$ (C=C) and $n−\pi*$ (C=O) transitions.[44] Similar to previously reported CQDs there is no resolved peak in the UV−vis spectrum corresponding to the maximum in the PL excitation spectrum (λ = 360 nm).[22] The PL emission profile shows typical excitation-wavelength-dependent behavior; on shifting the excitation wavelength from λ = 360 to 460 nm the emission maximum is shifted from λ = 464 to 532 nm. While the origin of PL luminescence in CQDs is not well understood, the prevailing view is that emission results from radiative recombination at surface-confined defect states.[35,45] The excitation-wavelength-dependent behavior is thought to be due to heterogeneity of such
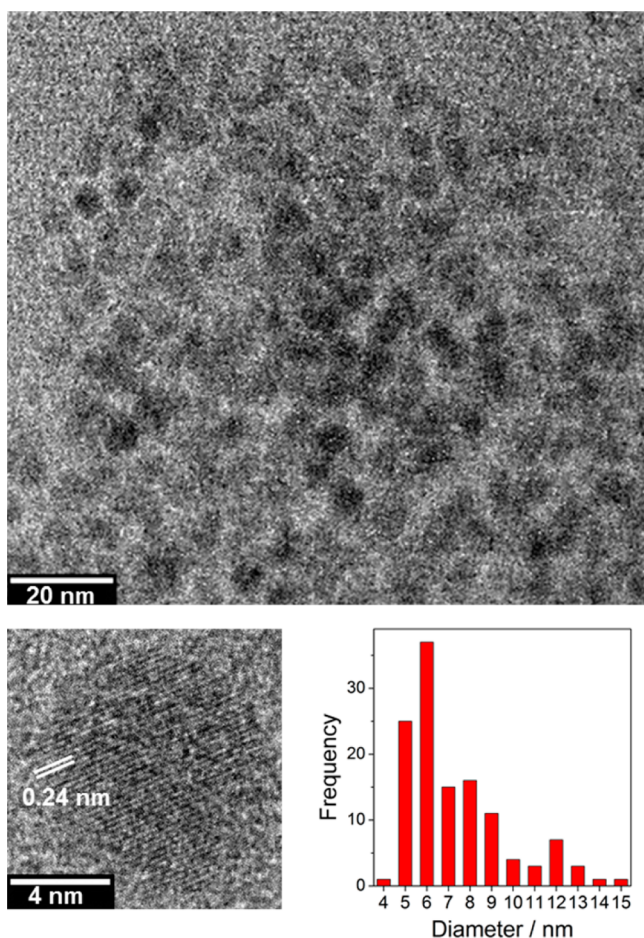
Figure 2. TEM images of CQDs at low magnification (top) showing the distribution of nanoparticle sizes (right, bottom) and at high magnification (left, bottom) showing a single particle and the graphitic spacing of the crystalline region.

Figure 3. UV−vis spectra of a solution of CQDs (0.5 mg mL^{-1}) and methyl viologen dichloride (MV^{2+}, 40 μM) in aqueous EDTA (0.1 M, pH 6) recorded every 2 min under full solar spectrum irradiation at 1 sun intensity; the inset shows a photograph of the solution before and after irradiation for 10 min.

emissive states in the sample from either multiple emission sites on each dot or different emissive sites between individual dots.[41,46] The PL quantum yield of 2.3% measured at an excitation wavelength of $\lambda = 360$ nm falls within the previously reported range for carboxylic acid terminated CQDs synthesized by hydrothermal methods.[22,29,41]

We investigated the electron transfer capabilities and reducing power of the CQDs by probing the photoreduction of methyl viologen (MV^{2+}; $E^{\circ\prime} = -0.45$ V vs NHE)[47] and its ability to quench photoluminescence. A solution of CQDs in aqueous ethylenediaminetetraacetic acid (EDTA, 0.1 M, pH 6) was irradiated in the presence of MV^{2+} under N$_2$ for 10 min. After 1 min of irradiation, peaks at $\lambda = 395$ and 603 nm corresponding to the reduced viologen species (MV$^{+\bullet}$)[48] begin to appear in the UV−vis spectrum, and after 10 min, there is a color change of the solution from yellow-brown to blue indicating formation of MV$^{+\bullet}$ (Figure 3). Quenching of CQD fluorescence by MV^{2+} was also observed further indicating photoelectron transfer to the MV^{2+} acceptor (Figure S7). The ability of the CQDs to photoreduce MV^{2+} demonstrates that the CQDs have sufficient reducing potential ($E^{0\prime} < -0.45$ V vs NHE) for proton reduction ($E^{\circ\prime} = -0.354$ V vs NHE at pH 6) and promising electron transfer properties for photocatalysis.

Figure 1 shows a schematic view of the CQD−molecular catalyst system for the solar-light driven production of H$_2$ from water. We have selected an ultra-abundant photosensitizer
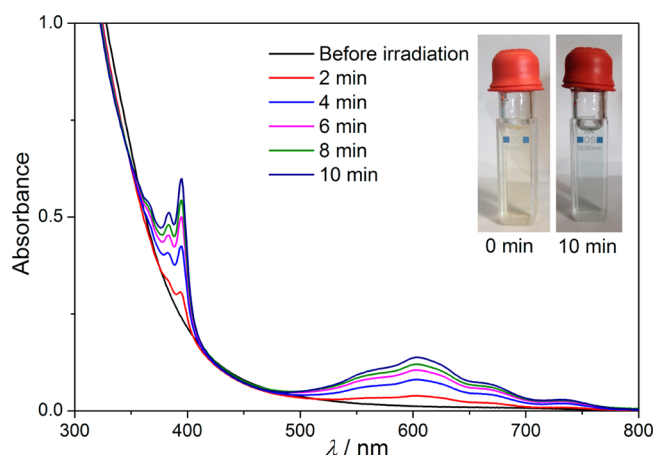
(CQD) in conjunction with a non-noble metal molecular H$_2$ evolution catalyst to produce a low cost and environmentally benign route to the solar fuel H$_2$ under mild (close to pH neutral) conditions. Synthetic molecular catalysts of first row transition metals are of interest as inexpensive alternatives to benchmark proton reduction catalysts such as platinum and hydrogenases, which suffer from high cost and, in the latter case, instability.[49] Synthetic molecular catalysts allow for bioinspired design and can be tuned for selectivity and tolerance to catalyst poisoning.[50] The recently reported bioinspired nickel bis(diphosphine) complex **NiP** (Figure 1) was selected as the catalyst for this system and was synthesized as described previously.[5] Complexes of this type are among the most active non-noble metal H$_2$ evolution catalysts in acidic organic[51,52] and aqueous solutions,[5,7] with a low overpotential requirement for the reduction of protons in water (approximately 0.2 V).[5] Furthermore, **NiP** is known to operate as a catalyst in homogeneous schemes with a ruthenium dye and in hybrid systems with nanoparticulate light absorbers during solar light irradiation.[5,7]

The photocatalytic systems were assembled by dissolving CQDs and **NiP** in an aqueous solution of sacrificial electron donor buffer (typically 0.1 M, 3 mL) in a glass photoreactor (total volume 7.74 mL). The vessel was purged with an inert gas containing an internal gas chromatography (GC) standard (2% CH$_4$ in N$_2$), sealed, and then irradiated using a solar light simulator (AM1.5G) at 1 sun intensity (100 mW cm^{-2}, unless otherwise stated). The headspace H$_2$ gas was periodically monitored by GC (see Experimental Section for details).

The parameters of the system (amount of CQD, amount of **NiP**, identity of sacrificial electron donor and pH of the solution) were varied systematically to produce a data set to optimize the H$_2$ production per catalyst and per CQD (Figures 4, S8−S9 and Tables S1−S3). Initially, several electron donors were screened to select a suitable match (Figure S8). EDTA was found to be the most active electron donor tested, although some activity was also observed with triethanolamine (TEOA) and ascorbic acid (AA). Importantly, negligible activity is obtained using citric acid (CA) as a potential donor, demonstrating that only the synthesized CQDs and not residual CA contribute to photocatalytic H$_2$ production.
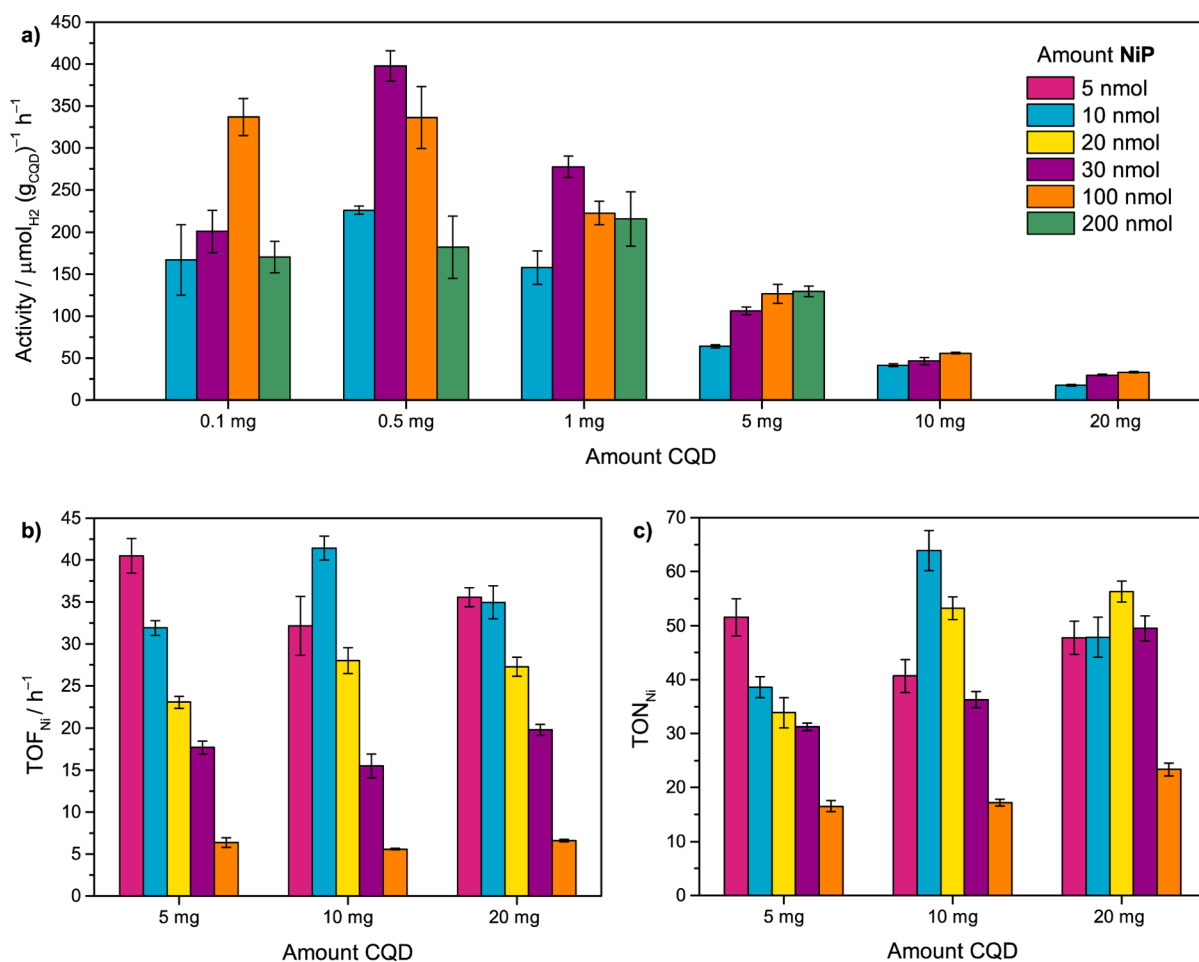
Figure 4. Photo-H_2 generation plotted as (a) activity, (b) TOF_{Ni}, and (c) TON_{Ni} (determined after 4 h irradiation) using various amounts of CQDs (0.1–20 mg) and **NiP** (5–200 nmol) in aqueous EDTA solution (0.1 M, pH 6) under full solar spectrum irradiation (AM 1.5G, 100 mW cm^{-2}).

Activity with EDTA as donor was then optimized against pH, where pH 6 was found to give both the highest initial activity and the maximum turnover of the system (Figure S9).

An optimized standard condition giving the highest turnover with respect to the Ni catalyst was achieved using 10 mg (corresponding to approximately 44 nmol) of CQD and 10 nmol of **NiP** in 0.1 M EDTA solution at pH 6. A TOF_{Ni} of 41 (mol_{H2}) $(mol_{NiP})^{-1}$ h^{-1} and TON_{Ni} after 4 h of 64 (mol_{H2}) $(mol_{NiP})^{-1}$ was achieved under these conditions with full solar spectrum light irradiation (Figures 4 and 5). Higher activity with respect to photosensitizer was obtained with increased catalyst loading. The highest tested activity of 398 μmol_{H2} $(g_{CQD})^{-1}$ h^{-1} was achieved with 0.5 mg (2.2 nmol) of CQD and 30 nmol of **NiP** (Figure 4).

The catalytic performance of **NiP** is in broad agreement with previously reported photocatalytic hybrid systems in water. In combination with a tris(bipyridine)ruthenium dye a TOF_{Ni} up to 460 (mol_{H2}) $(mol_{NiP})^{-1}$ h^{-1} was observed in solution and heterogeneous photosensitizers such as ruthenium dye-sensitized TiO$_2$ and CN$_x$ resulted in a TOF_{Ni} of 72 and 109 h^{-1}, respectively.[5,7] A photocatalytic system utilizing a similar nickel bis(diphosphine) catalyst together with a light-absorbing organic hydrogel showed a TOF_{Ni} of 19 h^{-1}.[53] The CQD–**NiP** system also compares well to the system of a phosphonated cobaloxime immobilized on ruthenium dye-sensitized TiO$_2$ (TOF_{Co} = 19 h^{-1}),[6] and the same cobaloxime in combination with the photounstable organic dye Eosin Y (TOF_{Co} = 62

h^{-1}).[12] Another cobalt containing molecular catalyst produced a TOF_{Co} of 4 h^{-1} with Eosin Y and 22 h^{-1} in an Eosin Y–TiO$_2$ hybrid system.[13] All of the systems containing molecular dyes were limited by photodegradation of the dye after a few hours, in contrast to CQDs (see below). Furthermore, none of the light absorbers listed above can compete with CQDs in terms of scalability and low cost.

In the absence of any of the components of the system— CQD (light absorber), **NiP** (catalyst), or EDTA (electron donor)—H$_2$ evolution did not occur (Figure 5). This confirms that the CQDs are not catalytic for proton reduction and do themselves not act as a sacrificial electron donor by auto-oxidation. Irradiation of CQDs results in absorption of light and the direct transfer of photoexcited electrons to the catalyst **NiP**, which carries out reduction of aqueous protons. The electron donor EDTA carries out quenching of photoinduced holes in the CQDs (Figure 1).

No induction phase was observed for photo-H$_2$ evolution with CQD–**NiP**, and upon replacement of the **NiP** in the system with NiCl$_2$, CoCl$_2$, and FeCl$_2$, no photoactivity was observed in either TEOA or EDTA solutions (Figures 5 and S10). These experiments, together with the observation that photoactivity of CQD–**NiP** ceases after several hours without readdition of the catalyst (see below), suggest that **NiP** is not acting as a precursor for the deposition of a heterogeneous catalyst, as has been observed or suspected for other systems with molecular catalysts.[54] Interestingly, even the use of a
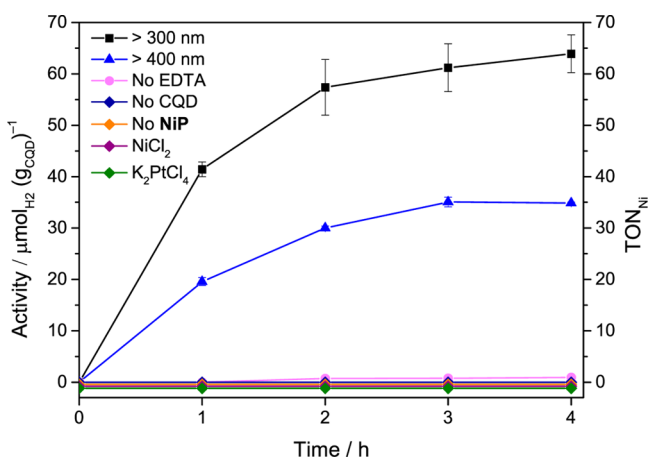
Figure 5. Optimized H_2 generation using CQD (10 mg) and **NiP** (10 nmol) in aqueous EDTA solution (0.1 M, pH 6) under 1 sun irradiation in the absence ($\lambda > 300$ nm) and presence of a 400 nm UV filter. Control experiments without EDTA, CQD, **NiP**, as well as with heterogeneous catalyst precursors, $NiCl_2$ (30 nmol) and K_2PtCl_4 (128 nmol, 0.5 wt %), are also shown.

Figure 6. Photocatalytic H_2 generation using CQD (10 mg) and **NiP** (10 nmol) in aqueous EDTA solution (0.1 M, pH 6) under 1 sun full solar spectrum irradiation. Activity is recovered upon each readdition of the catalyst, **NiP** (10 nmol), but not upon readdition of CQDs (10 mg).

standard platinum precursor solution (K_2PtCl_4 in 0.1 M TEOA or EDTA solution) with CQDs did not yield any detectable H_2 evolution (Figures 5 and S10). When using heterogeneous materials such as TiO_2 and CN_x as the light absorber, photodeposition of metallic Pt (a highly efficient precious-metal H_2 evolution catalyst) from the precursor K_2PtCl_4 under solar light irradiation results in an active system, though often with an induction period allowing for photodeposition of the metal catalyst.[16] A possible explanation for these observations is that the carboxylate-capped surface of the CQDs is not favorable for deposition of a heterogeneous catalyst. Another noteworthy possibility is that charge transfer dynamics could be limited by an unfavorably close proximity between a deposited metal catalyst and the CQD surface. A better matched spacing between a molecular catalyst core and the CQD surface may increase the charge separation lifetimes at the CQD−catalyst interface.[55] Further studies are currently ongoing in our laboratory to improve our understanding of this unique example, where a molecular catalyst not only outperforms conventional materials-based catalysts but is required for any activity at all.

Stability of the system was thought to be largely limited by the stability of the molecular catalyst with the rate decreasing each hour until, after 6 h, H_2 evolution is negligible. Readdition of the same quantity of fresh **NiP** catalyst (10 nmol) after each 6 h irradiation period confirmed this hypothesis (Figure 6) and is consistent with previous reports of short catalyst lifetimes in photocatalytic systems.[5,7,12] Reactivation is observed upon each readdition of **NiP**, and a repeating pattern of resumed activity followed by gradual decay of the catalyst occurs. Conversely, if the same quantity of fresh CQD (10 mg) is readded to the inactive solution following 6 h of irradiation, H_2 production does not resume. This result confirms both that the catalyst is the limiting factor of the stability and also that the CQDs have good photostability in this system (greater than 24 h).

The CQD−**NiP** photosystem was also tested under UV-free solar light by using a longpass filter ($\lambda > 400$ nm), which gave a TOF_{Ni} of 20 h^{-1}, corresponding to 50% of that under full solar spectrum (UV−visible) irradiation (Figure 5). This accords with the lower level of light absorption by the CQDs in the $\lambda >$
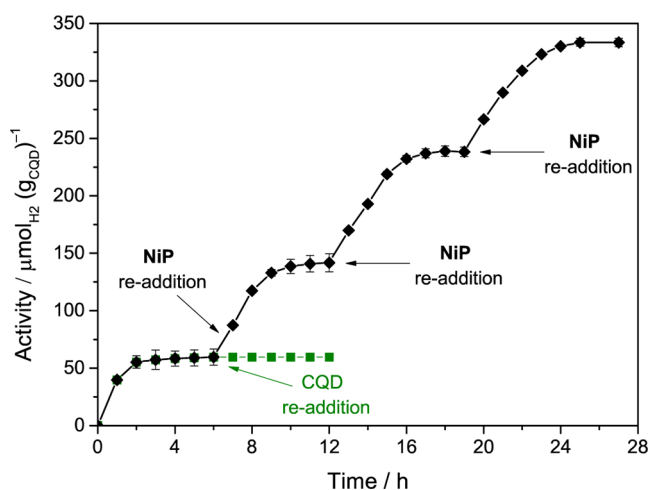
400 nm region (Figure S6). Activity persists (at a decreasing level) well into the visible light region leading to a TOF_{Ni} of 5 h^{-1} recorded with a $\lambda > 455$ nm longpass filter in place (Figure S11). The visible light response of the CQD−**NiP** system is considerably improved compared to the previously reported CN_x−**NiP** system where only 16% of the full spectrum activity was maintained with visible-light-only irradiation and negligible amounts of H_2 evolved with irradiation at $\lambda > 455$ nm.[7]

Light intensity was varied in order to gain insight into other possible performance limiting factors of the CQD−**NiP** system. Decreasing the light intensity by 50% and 80% using neutral density filters resulted in an almost linear decrease in TOF_{Ni} after 1 h, showing that the initial activity of the system is proportional to, and therefore dependent on, light intensity (Figure S12). However, the TON_{Ni} observed after 4 h decreases sublinearly with light intensity, since the decay of the catalyst becomes dominant in this time frame. The faster the initial rate (i.e., higher TOF_{Ni}), the faster the subsequent rate of decay of catalytic activity, suggesting that the decomposition of the catalyst is partly the result of over-reduction of the catalyst (i.e., **NiP** receives electrons faster than it can turn over).

Photoinactivation of the catalyst **NiP** also limits the overall stability of the CQD−**NiP** system as demonstrated by UV−vis spectroscopy and solar light experiments (Figure S13). Under full solar spectrum irradiation in the absence of CQD, the **NiP** band at $\lambda = 330$ nm is reduced in intensity over time, indicating that the catalyst is photounstable under these conditions. By contrast, when left in the dark or under visible-only ($\lambda > 400$ nm) irradiation, **NiP** showed relatively good stability in EDTA solution. This indicates that the **NiP** absorption at $\lambda = 330$ nm is responsible for its decomposition under these conditions. In agreement, the photo-H_2 generation using **NiP** that had been preirradiated with full solar spectrum light ($\lambda > 300$ nm) for 4 h prior to addition of CQDs showed significantly reduced activity and lifetime (Figure S13). When **NiP** is preirradiated with only visible light ($\lambda > 400$ nm) the photo-H_2 generation is comparable to the standard condition, demonstrating the photostability of **NiP** under visible light. Given that **NiP** is photostable under visible light irradiation and yet the activity of

the system still decays over time when irradiated with a $\lambda > 400$ nm filter (Figure S11), the loss of activity must be due to decomposition of **NiP** during the catalytic cycle. Thus, the lifetime of CQD−**NiP** under UV−vis irradiation is limited by **NiP** through decomposition during catalytic turnover and UV-light driven photodegradation.

The internal quantum efficiency (IQE) of the system was determined by equipping the solar light simulator with a narrow bandpass filter ($\lambda = 360 \pm 10$ nm, $I = 2.40$ mW cm^{-2}). An IQE of (1.40 ± 0.08) % was obtained using 0.5 mg CQD and 30 nmol of **NiP** in 3 mL of 0.1 M EDTA solution at pH 6. This efficiency is higher than previously reported noble-metal free systems such as CN$_x$−**NiP** (0.37 ± 0.02) %[7] and can be improved upon by identifying catalyst−CQD combinations with faster electron transfer and turnover to increase activity.

CONCLUSIONS

We have reported a photocatalytic H$_2$ production system using CQDs as a photosensitizer in combination with a molecular H$_2$ evolution Ni catalyst, a hybrid system consisting of only Earth-abundant materials with photoactivity in aqueous solution. Our results more widely demonstrate the potential use of CQDs in photocatalytic schemes, whereby they can absorb UV and visible light and directly transfer photoexcited electrons to solution based molecular electron acceptors and catalysts. Maximum activity with respect to CQD of 398 μmol$_{H_2}$ (g$_{CQD}$)$^{-1}$ h^{-1} and a TOF$_{Ni}$ of 41 h^{-1} optimized for **NiP** were achieved through parameter optimization under full solar spectrum light irradiation at 1 sun intensity. The activity parallels that of previously reported dye−catalyst hybrid systems but offers substantial benefits through the use of CQDs as photosensitizers, which are abundant, cheap, nontoxic, stable, and sustainably synthesized on a large scale. The loss of activity of the system was demonstrated to be due to instability of the molecular catalyst (both photoinstability and decomposition during catalytic turnover), whereas the CQDs themselves display a photostability of more than 24 h, thereby offering a significant advantage over rapidly photo-degrading molecular dye systems in aqueous solution. Identification of molecular catalysts compatible with this system but with greater stability is required to fully explore the long-term stability of CQDs for photocatalytic H$_2$ production. This work also demonstrates the necessity for active and stable molecular catalysts for use in such systems where heterogeneous catalysts and their precursors produce no activity.

EXPERIMENTAL SECTION

Materials. Reagents used throughout this work were obtained from commercial suppliers and used as received. Laboratory grade reagents were used in all synthetic procedures and chemicals for the analytical part of the work were of the highest available purity. Millipore water (18.2 MΩ cm @ 25 °C) was used throughout this work in both synthetic and analytical procedures. Buffer solutions were made using analytical grade reagents and titrated to the desired pH, as determined by a pH electrode (Mettler Toledo; SevenEasy) using NaOH. **NiP** was synthesized and characterized as previously described.[5]

Synthesis of CQDs. Water-soluble CQDs were synthesized using a modified literature procedure.[28] Citric acid (100 g) was thermolyzed (Carbolite furnace; ELF11/14B) under air at 180 °C for 40 h producing carboxylic acid capped CQDs as an orange-brown high-viscosity liquid. The previously reported heating time of 2.5 h was found to be insufficient for completion of the reaction, and furthermore, the reported purification step (to remove residual citric

acid) of dialysis using 2K-MWCO tubing proved ineffective as the CQDs freely permeated this membrane. Initially the citric acid melts forming a colorless liquid, which degasses with subsequent gradual color change through yellow and orange to brown. Upon cooling an orange-brown high-viscosity liquid is obtained, which was stirred with deionized water (100 mL) and an aqueous NaOH solution (5 M, 50 mL) to dissolve. More aqueous NaOH solution (5 M, approximately 25 mL) was subsequently added to neutralize the acidic CQDs to pH 7 resulting in an orange-brown solution of sodium carboxylate capped CQDs. As sufficient heating time was given to allow completion of the reaction, residual citric acid was not detected in the sample (by FT-IR, ^{13}C NMR and ion chromatography) and further purification was therefore not required. The product was isolated as a yellow-orange powder by freeze-drying (yield: 45 g from 100 g starting material).

Physical Characterization Techniques. High-resolution transmission electron microscopy (HR-TEM) images of the CQDs were recorded on a JEOL 3011 high resolution transmission electron microscope operating at an accelerating voltage of 300 kV. Particle size distribution analysis was carried out by counting 124 particles from six different images. The average molecular weight of the CQDs was calculated using the measured average diameter of 6.8 nm by assuming a perfect spherical shape and the density of graphitic carbon of 2.25 g cm^{-2}.[56] The resulting molecular weight is approximately 225 kDa.

Fourier transform infrared spectroscopy (FT-IR) was carried out on a Thermo Scientific Nicolet iS50 FT-IR spectrometer operating in ATR mode. ^{13}C {^{1}H} NMR spectra were taken using a Bruker 400 MHz spectrometer. Phase analysis of the CQDs was carried out using powder X-ray diffraction (XRD; X'Pert PRO, PANalytical BV).

UV−visible spectroscopy was carried out on a Varian Cary 50 UV−vis spectrophotometer using quartz cuvettes. Photoluminescence spectroscopy was carried out on an Agilent Technologies Cary Fluorescence Spectrophotometer. The CQD PL quantum yield (Φ_{CQD}) at an excitation wavelength of 360 nm was calculated according to the following equation using quinine in 0.1 M H$_2$SO$_4$ as a standard:

$$\Phi_{CQD} = \Phi_{Std}\left(\frac{G_{CQD}}{G_{Std}}\right)\left(\frac{\eta_{CQD}}{\eta_{Std}}\right)^2$$

where Φ_{Std} is the known PL quantum yield of quinine sulfate (54%),[57] G_{CQD} and G_{Std} are the gradients of the plot of integrated fluorescence vs absorbance at the excitation wavelength for CQDs and quinine sulfate, respectively, and η is the refractive index of the solvent.

X-ray photoelectron spectra (XPS) were obtained at the National EPSRC XPS User's Service (NEXUS) at Newcastle University, UK, an EPSRC Mid-Range Facility. Analysis was performed using a K-Alpha (Thermo Scientific, East Grinstead, UK) spectrometer utilizing a monochromatic Al Kα X-ray source (1486.6 eV, 400 μm spot size, 36 W). Survey spectra were collected with a pass energy of 200 eV and 3 sweeps, while high resolution spectra were collected at a pass energy of 40 eV with 10 sweeps. Measurements were taken at 3 points on each sample surface to ensure consistency, and charge neutralization was used throughout the analysis. CQD samples were dropcast from aqueous solution onto fluorine-doped tin oxide coated glass (conductive support) and oven-dried.

Photocatalysis Experiments. Typical photocatalytic experiments were set up as follows. Aqueous solutions containing an electron donor, CQDs, and the catalyst were added to borosilicate glass vials with a magnetic stir bar (total volume 7.74 mL) and sealed with a septum (Subaseal). The vessels were purged with an inert gas containing a gas chromatography (GC) standard (2% CH$_4$ in N$_2$) for at least 15 min prior to experiments. The vials were then placed in a thermoregulated rack at 25 °C with stirring and irradiated using a Xe lamp (Newport Oriel Solar Light Simulator; 100 mW cm^{-2}, 1 sun intensity) with an air mass 1.5 global (AM 1.5G) filter in the absence or presence of longpass (UV cutoff) or neutral density filters (UQG Optics). For H$_2$ detection, a gas chromatograph (Agilent 7890A Series) set up with a 5 Å molecular sieve column and a thermal conductivity detector (TCD) was employed. The GC oven was held at a constant temperature of 45 °C, and N$_2$ was used as the carrier gas.

Approximately 20 μL aliquots of headspace gas were removed from the reaction vessel using a gastight syringe (Hamilton; GASTIGHT). The H_2 produced was quantified by comparison to the CH_4 internal standard, and each measurement was carried out in triplicate. The solar light source and the gas chromatograph were calibrated regularly to ensure reproducibility.

Treatment of Data. All analytical measurements were performed in triplicate. The data were treated as follows: for a sample of n observations x_i, the unweighted mean value x and the standard deviation σ were calculated using the equations:

$$x_0 = \sum_i \frac{x_i}{n} \qquad \sigma = \sqrt{\sum_i \frac{(x_i - x_0)^2}{(n-1)}}$$

Turnover frequency determined after 1 h irradiation (TOF_{Ni}) and number (TON_{Ni}) with respect to the catalyst are expressed in the units $(mol_{H2})\,(mol_{NiP})^{-1}\,h^{-1}$ and $(mol_{H2})\,(mol_{NiP})^{-1}$, respectively. Activity with respect to the CQDs is expressed in the units $(\mu mol_{H2})\,(g_{CQD})^{-1}\,h^{-1}$.

Internal Quantum Efficiency (IQE) Measurement. H_2 production was carried out on the solar light simulator equipped with a narrow bandpass filter (Thor Laboratories) to provide a monochromatic light source at $\lambda = 360 \pm 10$ nm ($I = 2.40$ mW cm^{-2}). The IQE is then calculated using the following formula:

$$\text{IQE (\%)} = \frac{(2 \cdot n_{H2} \cdot N_A \cdot h \cdot c)}{(t_{irr} \cdot \lambda \cdot I \cdot A \cdot \alpha)} \cdot 100$$

where n_{H2} is the moles of photogenerated hydrogen, t_{irr} is the irradiation time, A is the irradiation cross-section, α is the percentage absorption of the incident light, and N_A, h, and c are Avogadro's constant, the Planck constant, and the speed of light, respectively.

■ ASSOCIATED CONTENT

ⓢ Supporting Information

Supporting figures and tables are included in the Supporting Information. The Supporting Information is available free of charge on the ACS Publications website at DOI: 10.1021/jacs.5b01650.

■ AUTHOR INFORMATION

Corresponding Author

*reisner@ch.cam.ac.uk

Author Contributions

†B.C.M.M. and G.A.M.H. contributed equally.

Notes

The authors declare no competing financial interest.

■ ACKNOWLEDGMENTS

■ REFERENCES

(1) Luo, J.; Im, J.-H.; Mayer, M. T.; Schreier, M.; Nazeeruddin, M. K.; Park, N.-G.; Tilley, S. D.; Fan, H. J.; Grätzel, M. *Science* **2014**, *345*, 1593−1596.

(2) McKone, J. R.; Lewis, N. S.; Gray, H. B. *Chem. Mater.* **2014**, *26*, 407−414.

(3) Tachibana, Y.; Vayssieres, L.; Durrant, J. R. *Nat. Photonics* **2012**, *6*, 511−518.

(4) Teets, T. S.; Nocera, D. G. *Chem. Commun.* **2011**, *47*, 9268−9274.

(5) Gross, M. A.; Reynal, A.; Durrant, J. R.; Reisner, E. *J. Am. Chem. Soc.* **2014**, *136*, 356−366.

(6) Lakadamyali, F.; Reisner, E. *Chem. Commun.* **2011**, *47*, 1695−1697.

(7) Caputo, C. A.; Gross, M. A.; Lau, V. W.; Cavazza, C.; Lotsch, B. V.; Reisner, E. *Angew. Chem. Int. Ed.* **2014**, *53*, 11538−11542.

(8) Han, Z.; Qui, F.; Eisenberg, R.; Holland, P. L.; Krauss, T. D. *Science* **2012**, *338*, 1321−1324.

(9) Wen, F.; Li, C. *Acc. Chem. Res.* **2013**, *46*, 2355−2364.

(10) Tran, P. D.; Wong, L. H.; Barber, J.; Loo, J. S. C. *Energy Environ. Sci.* **2012**, *5*, 5902−5918.

(11) Wilker, M. B.; Shinopoulos, K. E.; Brown, K. A.; Mulder, D. W.; King, P. W.; Dukovic, G. *J. Am. Chem. Soc.* **2014**, *136*, 4316−4324.

(12) Lakadamyali, F.; Kato, M.; Muresan, N. M.; Reisner, E. *Angew. Chem. Int. Ed.* **2012**, *51*, 9381−9384.

(13) Yin, M.; Ma, S.; Wu, C.; Fan, Y. *RSC Adv.* **2015**, *5*, 1852−1858.

(14) Smith, I. C.; Hoke, E. T.; Solis-Ibarra, D.; McGehee, M. D.; Karunadasa, H. I. *Angew. Chem. Int. Ed.* **2014**, *53*, 11232−11235.

(15) Niu, G.; Li, W.; Meng, F.; Wang, L.; Dong, H.; Qiu, Y. *J. Mater. Chem. A* **2014**, *2*, 705−710.

(16) Wang, X.; Maeda, K.; Thomas, A.; Takanabe, K.; Xin, G.; Carlsson, J. M.; Domen, K.; Antonietti, M. *Nat. Mater.* **2009**, *8*, 76−80.

(17) Kuriki, R.; Sekizawa, K.; Ishitani, O.; Maeda, K. *Angew. Chem. Int. Ed.* **2015**, *54*, 2406−2409.

(18) Cao, L.; Wang, X.; Meziani, M. J.; Lu, F.; Wang, H.; Luo, P. G.; Lin, Y.; Harruff, B. A.; Veca, L. M.; Murray, D.; Xie, S.-Y.; Sun, Y.-P. *J. Am. Chem. Soc.* **2007**, *129*, 11318−11319.

(19) Ding, C.; Zhu, A.; Tian, Y. *Acc. Chem. Res.* **2014**, *47*, 20−30.

(20) Wang, F.; Chen, Y.; Liu, C.; Ma, D. *Chem. Commun.* **2011**, *47*, 3502−3504.

(21) Wang, K.; Gao, Z.; Gao, G.; Wo, Y.; Wang, Y.; Shen, G.; Cui, D. *Nanoscale Res. Lett.* **2013**, *8*, 122−131.

(22) Baker, S. N.; Baker, G. A. *Angew. Chem. Int. Ed.* **2010**, *49*, 6726−6744.

(23) Lim, S. Y.; Shen, W.; Gao, Z. *Chem. Soc. Rev.* **2015**, *44*, 362−381.

(24) Tian, L.; Ghosh, D.; Chen, W.; Pradhan, S.; Chang, X.; Chen, S. *Chem. Mater.* **2009**, *21*, 2803−2809.

(25) For graphene-derived materials used in photocatalytic applications see: (a) Yeh, T.-F.; Syu, J.-M.; Cheng, C.; Chang, T.-H.; Teng, H. *Adv. Funct. Mater.* **2010**, *20*, 2255−2262. (b) Yeh, T.-F.; Teng, C.-Y.; Chen, S.-J.; Teng, H. *Adv. Funct. Mater.* **2014**, *26*, 3297−3303. (c) Yang, P.; Zhao, J.; Wang, J.; Cui, H.; Li, L.; Zhu, Z. *RSC Adv.* **2015**, *5*, 21332−21335.

(26) Liu, H.; Ye, T.; Mao, C. *Angew. Chem. Int. Ed.* **2007**, *46*, 6473−6475.

(27) Deng, J.; Lu, Q.; Mi, N.; Li, H.; Liu, M.; Xu, M.; Tan, L.; Xie, Q.; Zhang, Y.; Yao, S. *Chem.—Eur. J.* **2014**, *20*, 4993−4999.

(28) Guo, C. X.; Zhao, D.; Zhao, Q.; Wang, P.; Lu, X. *Chem. Commun.* **2014**, *50*, 7318−7321.

(29) Bourlinos, A. B.; Stassinopoulos, A.; Anglos, D.; Zboril, R.; Karakassides, M.; Giannelis, E. P. *Small* **2008**, *4*, 455−458.

(30) Yang, Z.-C.; Wang, M.; Yong, A. M.; Wong, S. Y.; Zhang, X.-H.; Tan, H.; Chang, A. Y.; Li, X.; Wang, J. *Chem. Commun.* **2011**, *47*, 11615−11617.

(31) Park, S. Y.; Lee, H. U.; Park, E. S.; Lee, S. C.; Lee, J.-W.; Jeong, S. W.; Kim, C. H.; Lee, Y.-C.; Huh, Y. S.; Lee, J. *ACS Appl. Mater. Interfaces* **2014**, *6*, 3365−3370.

(32) Liu, S.-S.; Wang, C.-F.; Li, C.-X.; Wang, J.; Mao, L.-H.; Chen, S. *J. Mater. Chem. C* **2014**, *2*, 6477−6483.

(33) Zhou, J.; Sheng, Z.; Han, H.; Zou, M.; Li, C. *Mater. Lett.* **2012**, *66*, 222−224.

(34) Strauss, V.; Margraf, J. T.; Dolle, C.; Butz, B.; Nacken, T. J.; Walter, J.; Bauer, W.; Peukert, W.; Spiecker, E.; Clark, T.; Guldi, D. M. *J. Am. Chem. Soc.* **2014**, *136*, 17308−17316.

(35) Wang, X.; Cao, L.; Lu, F.; Meziani, M. J.; Li, H.; Qi, G.; Zhou, B.; Harruff, B. A.; Kermarrec, F.; Sun, Y.-P. *Chem. Commun.* **2009**, *25*, 3774−3776.

(36) Tang, D.; Zhang, H.; Huang, H.; Liu, R.; Han, Y.; Liu, Y.; Tong, C.; Kang, Z. *Dalton Trans.* **2013**, *42*, 6285−6289.

(37) Yu, H.; Zhao, Y.; Zhou, C.; Shang, L.; Peng, Y.; Cao, Y.; Wu, L.-Z.; Tung, C.-H.; Zhang, T. *J. Mater. Chem. A* **2014**, *2*, 3344−3351.

(38) Wu, W.; Zhan, L.; Ohkubo, K.; Yamada, Y.; Wu, M.; Fukuzumi, S. *J. Photochem. Photobiol., B* **2015**, *in press*, doi: 10.1016/j.jphotobiol.2014.10.018.

(39) Cao, L.; Sahu, S.; Anilkumar, P.; Bunker, C. E.; Xu, J.; Shiral Fernando, K. A.; Wang, P.; Guliants, E. A.; Tackett, K. N.; Sun, Y.-P. *J. Am. Chem. Soc.* **2011**, *133*, 4754−4757.

(40) Sahu, S.; Liu, Y.; Wang, P.; Bunker, C. E.; Shiral Fernando, K. A.; Lewis, W. K.; Guliants, E. A.; Yang, F.; Wang, J.; Sun, Y.-P. *Langmuir* **2014**, *30*, 8631−8636.

(41) Ghosh, S.; Chizhik, A. M.; Karedla, N.; Dekaliuk, M. O.; Gregor, I.; Schuhmann, H.; Seibt, M.; Bodensiek, K.; Schaap, I. A. T.; Schulz, O.; Demchenko, A. P.; Enderlein, J.; Chizhik, A. I. *Nano Lett.* **2014**, *14*, 5656−5661.

(42) Peng, H.; Travas-Sejdic, J. *Chem. Mater.* **2009**, *21*, 5563−5565.

(43) Zhou, J.; Booker, C.; Li, R.; Zhou, X.; Sham, T.-K.; Sun, X.; Ding, Z. *J. Am. Chem. Soc.* **2007**, *129*, 744−745.

(44) Li, X.; Zhang, S.; Kulinich, S. A.; Liu, Y.; Zeng, H. *Sci. Rep.* **2014**, *4*, 4976.

(45) Cao, L.; Meziani, M. J.; Sahu, S.; Sun, Y.-P. *Acc. Chem. Res.* **2013**, *46*, 171−180.

(46) Sun, Y.-P.; Zhou, B.; Lin, Y.; Wang, W.; Shiral Fernando, K. A.; Pathak, P.; Meziani, M. J.; Harruff, B. A.; Wang, X.; Wang, H.; Luo, P. G.; Yang, H.; Kose, M. E.; Chen, B.; Veca, L. M.; Xie, S.-Y. *J. Am. Chem. Soc.* **2006**, *128*, 7756−7757.

(47) Bird, C. L.; Kuhn, A. T. *Chem. Soc. Rev.* **1981**, *10*, 49−82.

(48) Watanabe, T.; Honda, K. *J. Phys. Chem.* **1982**, *86*, 2617−2619.

(49) Sakai, T.; Mersch, D.; Reisner, E. *Angew. Chem. Int. Ed.* **2013**, *52*, 12313−12316.

(50) Wakerley, D. W.; Gross, M. A.; Reisner, E. *Chem. Commun.* **2014**, *50*, 15995−15998.

(51) Wilson, A. D.; Newell, R. H.; McNevin, M. J.; Muckerman, J. T.; Rakowski DuBois, M.; DuBois, D. L. *J. Am. Chem. Soc.* **2006**, *128*, 358−366.

(52) Helm, M. L.; Stewart, M. P.; Bullock, R. M.; Rakowski DuBois, M.; DuBois, D. L. *Science* **2011**, *333*, 863−866.

(53) Weingarten, A. S.; Kazantsev, R. V.; Palmer, L. C.; McClendon, M.; Koltonow, A. R.; Samuel, A. P. S.; Kiebala, D. J.; Wasielewski, M. R.; Stupp, S. I. *Nat. Chem.* **2014**, *6*, 964−970.

(54) Artero, V.; Fontecave, M. *Chem. Soc. Rev.* **2013**, *42*, 2338−2356.

(55) Reynal, A.; Willkomm, J.; Muresan, N. M.; Lakadamyali, F.; Planells, M.; Reisner, E.; Durrant, J. R. *Chem. Commun.* **2014**, *50*, 12768−12771.

(56) Pierson, H. O. *Handbook of carbon, graphite, diamonds and fullerenes: processing, properties and applications*; Noyes Publications: Park Ridge, New Jersey, 1993; p 98.

(57) Melhuish, W. H. *J. Phys. Chem.* **1961**, *65*, 229−235.